Large Amplitude Nonlinear Vibrations in Turning Processes

Z. Dombóvári[1], R. E. Wilson[2], G. Stépán[1]
[1]Department of Applied Mechanics, Budapest University of Technology and Economics, Hungary
[2]Department of Engineering Mathematics, University of Bristol, United Kingdom

Abstract
Self-excited nonlinear vibrations occurring in the machining processes are investigated in this paper. Our treatment applies analytical techniques to a one degree of freedom but strongly nonlinear mechanical model of the turning process. This tool enables us to describe and analyse the highly nonlinear dynamics of the appearing periodic and more complicated motions. Using normal form calculations for the delay-differential equation model, we prove that the low-amplitude vibrations are unstable all along the stability lobes due to the subcriticality of *Hopf bifurcations*. This means that self-excited vibrations of the machine tool may occur below the stability boundaries predicted by the linear theory. Zones of bi-stability are presented in the traditional stability lobe diagram.

Keywords:
orthogonal cutting, Hopf bifurcation, subcritical, bi-stable

1 INTRODUCTION

Nowadays, high speed cutting comes to the front due to high quality and economic requirements. The corresponding machine tools are expensive compared to the usual machines because of their complex structure. The so-called regenerative chatter is not just harmful for these machines, but it also has a negative effect on the machined surface quality. The regenerative effect is a kind of self-excited high-frequency vibration originated in the chip formation process [11, 12].

The stability of the regenerative vibrations has been studied extensively during the last decades [1, 7]. The study of the corresponding nonlinear vibrations started in the last ten years only [3, 8, 9]. These results led to the final conclusion that unstable vibrations exist in the vicinity of the otherwise stable stationary cutting in the stable parameter regions.

The parameter region where this situation can occur will be called region of bistability. The explanation of this terminology is that the unstable vibration separates two attractors in the sense of dynamical systems. Apart of the stable stationary cutting there must exist another attractor, that is, a large amplitude stable oscillation outside the unstable vibration. This large amplitude nonlinear vibration is stable in dynamical sense, but it is often called instability by the community of researchers working in production technology. Actually, these vibrations are of little interest from technology view-point.

However, the width of the bistable region is important: it defines that region in the stable parameter domain where the stable cutting process is more or less sensitive for perturbations like non-homogeneous work-piece material.

In this paper, we prove the existence of the unstable vibrations for a large set of cutting force characteristics. Also, the bistable domain is constructed in the parameter space of the technological parameters like cutting speed and chip width.

2 MODEL CONSTRUCTION

In order to investigate the fundamental effect of nonlinearity during cutting, we have to apply as simple model as possible. Our one degree of freedom (DOF) orthogonal cutting model (Figure 1) might be far from the real cutting conditions, but it will help to follow analytically the influence of the cutting parameters on the dynamical behaviour. The desired chip thickness h_0 equals to the feed per revolution and the chip width w corresponds to the depth of cut.

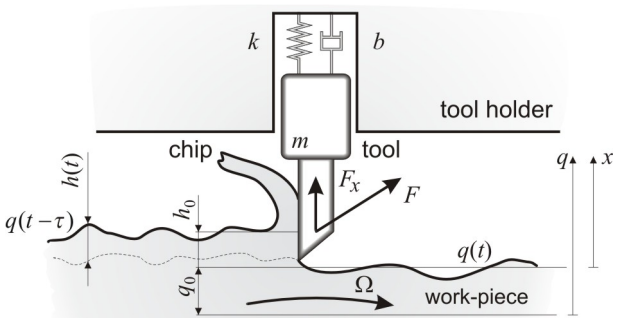

Figure 1: Orthogonal cutting with regenerative effect.

We disregard the geometric nonlinearities of the machine tool structure since their influences are far smaller than those of cutting force characteristics that exist on very small scale. Thus, the equation of motion of the chosen model assumes the form:

$$\ddot{q}(t) + 2\kappa\omega_n \dot{q}(t) + \omega_n^2 q(t) = \frac{1}{m} F_x(t)\,, \qquad (1)$$

where ω_n and κ are the natural angular frequency and the damping ratio of the essential vibration mode described by the general coordinate q that refers to the tool position. We can express these parameters with the modal mass m, stiffness k and the damping factor b.

$$\omega_n = \sqrt{\frac{k}{m}}\,,\ \kappa = \frac{b}{2\,m\,\omega_n}\,.$$

$F_x(t)$ is the essential component of the actual cutting force. Dot refers to time derivative.

2.1 Cutting force characteristics

To build up the dynamical model, we need a simple expression of the cutting force characteristics. There are a number of traditional, empirical formulas for the cutting force depending on the chip width and thickness. The most popular and generally applied one is the power-law [10]

$$F_x(h) = K\, w\, h^{\nu}, \quad K, \nu \in \mathbb{R}^+.$$

K and ν are empirical parameters. The exponent ν may vary from 2/5 [4] through 3/4 [5] to 4/5 [11]. The origin of these power-law expressions is in the linear optimisation techniques in the parameter space of the logarithms of the cutting parameters w and h.

There is a less frequently used expression of the cutting force which is essentially a cubic polynomial curve fitted on the experimental data [6]

$$F_x(h) = z_C\, w(\rho_1 h + \rho_2 h^2 + \rho_3 h^3),\ z_C \in \mathbb{Z},\ \rho_{1,2,3} \in \mathbb{R}. \quad (2)$$

(e.g., z_C = 4, ρ_1= $6.1096 \cdot 10^9$ [N/m^2], ρ_2= $-5.41416 \cdot 10^{13}$ [N/m^3], ρ_3= $2.03769 \cdot 10^{17}$ [N/m^4]; [6]). Originally, these measurement data were obtained for full immersion milling with a face mill with even number (z = 24) of teeth. For this case, the cutting process nearly corresponds to the orthogonal cutting since the parametric excitation can be averaged in the system.

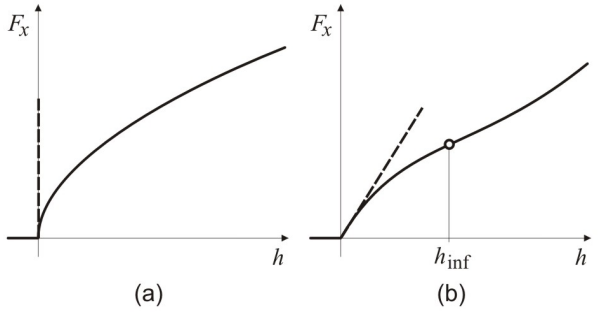

Figure 2: (a) and (b) show the curves of the power-law and the *Tobias cubic curve* cutting force characteristics.

From dynamical view-point, there are essential differences between the presented empirical interpretations of the cutting forces. The power-law in Figure 2 (a) has a vertical tangent at the origin, where the tool just touches the surface of the work-piece. This feature causes serious problems in the mathematical treatment of the loss of contact (e.g., uniqueness of solutions, uncertainties in numerical simulations). Also, the bifurcation calculations require *Taylor series* expansion of the power-law function at the stationary cutting.

In turn, the *Tobias cubic curve* Figure 2 (b) has a finite gradient at the origin and an inflection at

$$h_{\inf} = -\frac{1}{3}\frac{\rho_2}{\rho_3}, \quad (3)$$

while it has more parameters and so greater class of functions can be identified this way.

2.2 Equation of motion

As show in Figure 1, the so-called regenerative effect arises during the chip separation. Through the relative vibration between the tool and the work-piece, the tool leaves its motion pattern on the work-piece that excites the system after one revolution of the work-piece. The actual chip thickness can be expressed as a function of the present and the delayed motions of the tool

$$h(t) = q(t-\tau) - q(t) + h_0, \quad (4)$$

where h_0 is the theoretical chip thickness and $\tau = 2\pi/\Omega$ is the time delay which is equal to the time period of one revolution of the work-piece of angular velocity Ω. The chip thickness variation has the form

$$\Delta h(t) = h(t) - h_0 = q(t-\tau) - q(t).$$

The power series of the cutting force with respect to the chip thickness variation is given by

$$F_x(h(t)) = F_{x0} + k_1 \Delta h(t) + k_2 \Delta h^2(t) + k_3 \Delta h^3(t) + \ldots,$$

$$k_j = \frac{1}{j!}\frac{\partial^j F_x}{\partial h^j}\bigg|_{h_0}, \quad j \in \mathbb{N}^+.$$

Note that in the case of *Tobias cubic curve* this is a finite polynomial function of third degree.

Let us consider the perturbed system around the steady state solution with the new coordinate $x(t)$ defined by $q(t) = q_0 + x(t)$. With substitution into (1), we obtain $q_0 = F_{x0} / (m\, \omega_n^2)$ for the equilibrium, which is the static deformation of the tool.

Thus we can obtain the perturbed equation of motion:

$$\ddot{x}(t) + 2\kappa\omega_n \dot{x}(t) + \omega_n^2 x(t) = \frac{1}{m}(k_1 \Delta h(t) + k_2 \Delta h^2(t) + k_3 \Delta h^3(t)),$$

where

$$\Delta h(t) = q(t-\tau) - q(t) = x(t-\tau) - x(t).$$

After the introduction of the dimensionless time $\tilde{t} := \omega_n t$ we obtain a more general form

$$x''(\tilde{t}) + 2\kappa x'(\tilde{t}) + (1+\tilde{w})\, x(\tilde{t}) = \tilde{w}(x(\tilde{t}-\tilde{\tau}) + \eta_2 (x(\tilde{t}-\tilde{\tau}) - x(\tilde{t}))^2) + \tilde{w}\eta_3 (x(\tilde{t}-\tilde{\tau}) - x(\tilde{t}))^3,$$

where prime is the derivative with respect to $\tilde{t}$ and

$$\tilde{w} = \frac{k_1}{m\omega_n^2},\ k_1 = z_C w(\rho_1 + 2\rho_2 h_0 + 3\rho_3 h_0^2),$$

and the coefficients of the square and cubic terms in the nonlinear excitation are

$$\eta_2 = \frac{\rho_2 + 3\rho_3 h_0}{\rho_1 + 2\rho_2 h_0 + 3\rho_3 h_0^2}, \eta_3 = \frac{\rho_3}{\rho_1 + 2\rho_2 h_0 + 3\rho_3 h_0^2}. \quad (5)$$

By abuse of notation, we drop the tilde, thus, the equation of motion is

$$x''(t) + 2\kappa x'(t) + (1+w)\, x(t) = w(x(t-\tau) + \eta_2 (x(t-\tau) - x(t))^2 + \eta_3 (x(t-\tau) - x(t))^3). \quad (6)$$

In first order delayed differential equations (DDE) form we have

$$\mathbf{y}'(t) = \mathbf{L}\,\mathbf{y}(t) + \mathbf{R}\,\mathbf{y}(t-\tau) + \mathbf{g}(\mathbf{y}(t), \mathbf{y}(t-\tau)), \quad (7)$$

where $\mathbf{y} = \mathrm{col}\,(x(t),\ x'(t))$ and the linear non-delayed and delayed coefficient matrices and the nonlinear term are given by

$$\mathbf{L} = \begin{bmatrix} 0 & 1 \\ -(1+w) & -2\kappa \end{bmatrix}, \quad \mathbf{R} = \begin{bmatrix} 0 & 0 \\ w & 0 \end{bmatrix},$$

$$\mathbf{g}(\mathbf{y}(t), \mathbf{y}(t-\tau)) = \begin{bmatrix} 0 \\ w\,\eta_2\,(x(t-\tau)-x(t))^2 \\ \qquad + w\eta_3\,(x(t-\tau)-x(t))^3 \end{bmatrix}.$$

2.3 Operator formulation

In order to investigate the nonlinear DDE, we transform the system into the space of continuously differentiable functions by the shift,

$$\mathbf{u}_t(\theta) = \mathbf{u}(t+\theta) : [-\tau, 0] \to \mathbb{R}^2, \qquad \theta \in [-\tau, 0].$$

In this space the whole system can be rewritten as an operational differential equation (OpDE)

$$\mathbf{y}_t' = \mathcal{A}\,\mathbf{y}_t + \mathcal{F}(\mathbf{y}_t), \tag{8}$$

with the linear operator $\mathcal{A}$ defined by

$$(\mathcal{A}\,\mathbf{y}_t)(\theta) = \begin{cases} \mathbf{y}_t^o(\theta), & \text{if } \theta \in [-\tau, 0), \\ \mathbf{L}\,\mathbf{y}_t(0) + \mathbf{R}\,\mathbf{y}_t(-\tau), & \text{if } \theta = 0, \end{cases} \tag{9}$$

and the nonlinear operator $\mathcal{F}$ defined by

$$(\mathcal{F}(\mathbf{y}_t))(\theta) = \begin{cases} \mathbf{0}, & \text{if } \theta \in [-\tau, 0), \\ \mathbf{g}(\mathbf{y}_t(0), \mathbf{y}_t(-\tau)), & \text{if } \theta = 0. \end{cases} \tag{10}$$

It can be shown that (8) corresponds to (7) since the two kinds of derivates are equivalent

$$\mathbf{u}_t^o := \frac{d}{d\theta}\mathbf{u}_t(\theta) = \frac{d}{dt}\mathbf{u}(t+\theta), \qquad \theta \in [-\tau, 0).$$

3 LINEAR STABILITY

Consider only the linear part $\mathbf{y}_t' = \mathcal{A}\,\mathbf{y}_t$ of (8) with the exponential trial solution:

$$\mathbf{y}_t(\theta) = \mathbf{b}(\theta)\,e^{\lambda t}, \ \theta \in [-\tau, 0], \ \ \lambda \in \mathbb{C}. \tag{11}$$

The trivial solution of (8) is exponentially stable if the characteristic exponents λ_k, that is, the eigenvalues of the linear operator $\mathcal{A}$ satisfy

$$\mathrm{Re}\,\lambda_k < 0, \ k \in \mathbb{N}^+.$$

With the substitution of the general solution into the linear equation, we get a boundary value problem

$$\mathbf{b}^o(\theta) = \lambda\,\mathbf{b}(\theta),$$

$$(\mathbf{L} - \lambda\,\mathbf{I})\,\mathbf{b}(0) + \mathbf{R}\,\mathbf{b}(-\tau) = \mathbf{0}.$$

With the trial solution $\mathbf{b}(\theta)$=$\mathbf{B}\ \exp(\lambda\,\theta)$, this leads to an eigenvalue problem leading to the characteristic function

$$\begin{aligned} D(\lambda) &= \det(\mathbf{L} - \lambda\,\mathbf{I} + \mathbf{R}\,e^{-\lambda\tau}) \\ &= \lambda^2 + 2\kappa\,\lambda + 1 + w - we^{-\lambda\tau}. \end{aligned} \tag{12}$$

The damping factor is fixed for a certain machine tool, so the stability chart will be constructed for the variable parameters w and τ, which are determined by the chip width and the cutting speed. The stability boundaries for these parameters are expressed as a function of the dimensionless vibration frequency ω after the substitution $\lambda = i\omega$:

$$\begin{aligned} w(\omega) &= \frac{(\omega^2-1)^2 + 4\kappa^2\omega^2}{2(\omega^2-1)}, \\ \tau(\omega) &= \frac{2}{\omega}\left(j\,\pi + \arctan\frac{1-\omega^2}{2\kappa\,\omega} \right), \ \ j \in \mathbb{N}. \end{aligned} \tag{13}$$

Then the dimensionless angular velocity Ω of the work-piece is calculated as

$$\Omega(\omega) = \frac{2\,\pi}{\tau(\omega)}. \tag{14}$$

The *jth* parametric function formed from (13) and (14) is called *jth* 'lobe'. The stability limit consists of the sections of the lobes in the (w, Ω) plane beneath which the cutting process is asymptotically stable [7, 12].

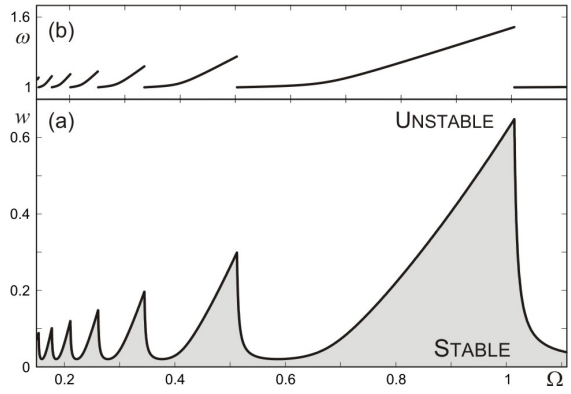

Figure 3: The linear stability chart (a) and the vibration frequency at the stability limits (b); κ=0.01.

4 NONLINEAR INVESTIGATION

At the stability limits, there are two complex conjugate critical characteristic roots. We will choose the dimensionless chip width w as a bifurcation parameter and follow the motion of these critical roots in the complex plane as w increases through the stability limit.

4.1 Overview of the Hopf bifurcation calculus

We briefly present here the procedure of the *Hopf bifurcation* calculation following the algorithm given in [2, 8].

Variation of critical eigenvalues

According to the *Hopf bifurcation theory* we need the derivates of the critical eigenvalues with respect to the bifurcation parameter w, which comes from the implicit differentiation of characteristic function (12):

$$\gamma(\omega) = \mathrm{Re}\left(\frac{d\,\lambda}{d\,w}\bigg|_{\lambda = i\,\omega} \right) = 2\,\frac{(\omega^2-1)^2}{w(\omega)}\,\frac{\gamma_n(\omega)}{\gamma_d(\omega)},$$

where

$$\gamma_n(\omega) = 4\kappa^2\,\tau(\omega)\,\omega^2 + 4\kappa(\omega^2+1) + \tau(\omega)(\omega^2-1)^2, \tag{15}$$

$$\begin{aligned}\gamma_d(\omega) = {} & 16\kappa^4\tau^2(\omega)\omega^4 + 32\kappa^3\tau(\omega)\,\omega^2(\omega^2-1) + \\ & 8\kappa\tau(\omega)\,(\omega^2-1)^2(1+3\omega^2) + \\ & 8\kappa^2(\omega^2-1)^2(2+\tau^2(\omega)\,\omega^2) + \\ & (\omega^2-1)^2(16\omega^2+\tau^2(\omega)\,(\omega^2-1)^2)\,.\end{aligned} \tag{16}$$

Centre Manifold

At the linear stability limit the *Hopf bifurcation* can be studied on a two dimensional centre manifold embedded in the infinite dimensional phase space. The tangent subspace of the centre manifold at the origin is spanned by the real and imaginary part of the critical eigenvectors of the linear operator $\mathcal{A}$ (Figure 4).

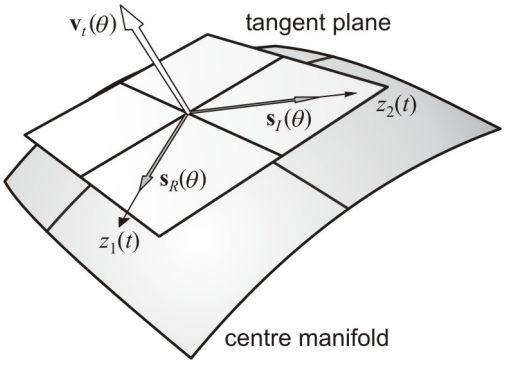

Figure 4: Tangent subspace and centre manifold at the steady state

The critical eigenvectors are calculated from

$$(\mathcal{A}\,\mathbf{s})(\theta) = i\,\omega\,\mathbf{s}(\theta)\,,\ \mathbf{s}(\theta) = \mathbf{s}_R(\theta) + i\,\mathbf{s}_I(\theta)\,.$$

Substituting the operator $\mathcal{A}$ according to (9), and solving the corresponding boundary value problem, we obtain the real and the imaginary part of the eigenvectors

$$\mathbf{s}_R(\theta) = \begin{bmatrix} \cos\omega\theta \\ -\omega\sin\omega\theta \end{bmatrix} \text{ and } \mathbf{s}_I(\theta) = \begin{bmatrix} \sin\omega\theta \\ \omega\cos\omega\theta \end{bmatrix}. \tag{17}$$

Since the base of the tangent space defined by (17) is not orthogonal, to make the projection, we need its reciprocal base spanned by $\mathbf{n}_R$ and $\mathbf{n}_I$, which satisfy the adjoint problem

$$(\mathcal{A}^*\mathbf{n})(\vartheta) = -i\omega\,\mathbf{n}(\vartheta)\,,\ \mathbf{n}(\vartheta) = \mathbf{n}_R(\vartheta) + i\,\mathbf{n}_I(\vartheta)\,, \tag{18}$$

where $\vartheta \in [0,\ \tau]$ and the adjoint operator $\mathcal{A}^*$ is defined as

$$(\mathcal{A}^*\mathbf{u})(\vartheta) = \begin{cases} \frac{d}{d\vartheta}\mathbf{u}(\vartheta), & \text{if } \vartheta \in (0,\tau], \\ \mathbf{L}^*\,\mathbf{u}(0) + \mathbf{R}^*\,\mathbf{u}(\tau), & \text{if } \vartheta = 0. \end{cases}$$

The orthonormality of the critical eigenvectors are prescribed by the conditions

$$(\mathbf{n}_R, \mathbf{s}_R) = 1\,,\ (\mathbf{n}_R, \mathbf{s}_I) = 0\,,$$

where the scalar product is defined by

$$(\mathbf{u}, \mathbf{v}) = \int_{-\tau}^{0} \mathbf{u}^*(\theta+\tau)\,\mathbf{R}\,\mathbf{v}(\theta)\,\mathrm{d}\theta + \mathbf{u}^*(0)\,\mathbf{v}(0)\,.$$

The solution of the linear boundary value problem (18) provides the critical normed adjoint eigenvectors

$$\begin{aligned}\mathbf{n}_R(\vartheta) &= \mathbf{b}_1(\omega)\cos\omega\vartheta - \mathbf{b}_2(\omega)\sin\omega\vartheta\,, \\ \mathbf{n}_I(\vartheta) &= \mathbf{b}_1(\omega)\sin\omega\vartheta + \mathbf{b}_2(\omega)\cos\omega\vartheta\,,\end{aligned} \qquad \vartheta \in [0,\ \tau]\,.$$

where the coefficient vectors $\mathbf{b}_1(\omega)$ and $\mathbf{b}_2(\omega)$ are not presented here. With the help of the new coordinates $\mathbf{z}(t) = \mathrm{col}(z_1(t),\, z_2(t))$ we can decompose the phase space in the following way:

$$\mathbf{y}_t(\theta) = z_1(t)\ \mathbf{s}_R(\theta) + z_2(t)\,\mathbf{s}_I(\theta) + \mathbf{v}_t(\theta) = (\mathcal{T}\,\mathbf{z})(\theta) + \mathbf{v}_t(\theta),$$

where the transformation operator is

$$(\mathcal{T}\,\mathbf{z})(\theta) = \left[\mathbf{s}_R(\theta)\ \vdots\ \mathbf{s}_I(\theta)\right]\mathbf{z}(t)\,,$$

and the corresponding projector operator will be

$$\mathcal{T}^p\,\mathbf{u}_t = [\,(\mathbf{n}_R, \mathbf{u}_t)\ \ (\mathbf{n}_I, \mathbf{u}_t)\,]^T\,,$$

consequently

$$\mathbf{z}(t) = \mathcal{T}^p\,\mathbf{y}_t\,.$$

With the new coordinates we can express the transformed OpDE as

$$\begin{bmatrix} \mathbf{z}'(t) \\ \cdots\cdots \\ \mathbf{v}_t'(\theta) \end{bmatrix} = \begin{bmatrix} \mathbf{J}_b & \vdots & 0 \\ \cdots & \cdots & \cdots \\ 0 & \vdots & \mathcal{A} \end{bmatrix} \begin{bmatrix} \mathbf{z}(t) \\ \cdots\cdots \\ \mathbf{v}_t(\theta) \end{bmatrix} + \begin{bmatrix} \mathcal{T}^p\,\mathcal{F}(\mathbf{z}(t),\, \mathbf{v}_t) \\ \cdots\cdots\cdots\cdots\cdots \\ \mathcal{G}(\mathbf{z},\, \mathbf{v}_t) \end{bmatrix}, \tag{19}$$

where

$$\mathcal{G}(\mathbf{z},\, \mathbf{v}_t) = \mathcal{F}(\mathbf{z},\, \mathbf{v}_t) - \mathcal{T}(\mathcal{T}^p\,\mathcal{F}(\mathbf{z},\, \mathbf{v}_t))\,,$$

and the *Jordan block* at the critical parameters assumes the form

$$\mathbf{J}_b = \begin{bmatrix} 0 & \omega \\ -\omega & 0 \end{bmatrix}.$$

The centre manifold is bent, so its second degree approximation with the new coordinates $\mathbf{z}(t)$ is

$$\begin{aligned}\mathbf{v}_t(\theta) &\approx \tilde{\mathbf{v}}(\theta, \mathbf{z}(t)) \\ &= \frac{1}{2}(\mathbf{h}_1(\theta)\,z_1^2(t) + \mathbf{h}_2(\theta)z_1(t)\,z_2(t) + \mathbf{h}_3(\theta)\,z_2^2(t))\,.\end{aligned}$$

where the unknown coefficient functions are calculated from a linear boundary value problem, again. During the lengthy calculations, the restriction of the nonlinear operator $\mathcal{F}$ (10) on the centre manifold requires the following substitution of the nonlinear function

$$\begin{aligned}\mathbf{g}(\mathbf{y}(t),\, \mathbf{y}(t-\tau)) &\approx \tilde{\mathbf{g}}(\mathbf{z}(t), \tilde{\mathbf{v}}(\bullet, \mathbf{z}(t))) \\ &= \frac{a(\mathbf{z}(t))}{w(\omega)} \begin{bmatrix} 0 \\ a(\mathbf{z}(t)) \left(\eta_2 + \dfrac{\eta_3}{w(\omega)}\,a(\mathbf{z}(t))\right) \\ \qquad + 2\,(\tilde{v}_1(-\tau, \mathbf{z}(t)) - \tilde{v}_1(0, \mathbf{z}(t))) \end{bmatrix},\end{aligned}$$

$a(\mathbf{z}(t)) = (1-\omega^2)\,z_1(t) + 2\kappa\omega\,z_2(t)$ and $\eta_2,\ \eta_3$ come from (5).

4.2 Poincaré-Ljapunov constant

The first two scalar equations of (19) describe the flow on the centre manifold, where the *Hopf bifurcation* takes place. Its second and third order terms assume the form

$$\begin{aligned}\mathcal{T}^p\,\mathcal{F}(\mathbf{z}(t),\, \mathbf{v}_t) &\approx \mathcal{T}^p\,\mathcal{F}(\mathbf{z}(t)\ \tilde{\mathbf{v}}(\bullet, \mathbf{z}(t))) \\ &= \begin{bmatrix} \sum_{j,k\geq 0,\ j+k=2,\ 3} a_{jk}\ z_1^j(t) z_2^k(t) \\ \sum_{j,k\geq 0,\ j+k=2,\ 3} b_{jk}\ z_1^j(t) z_2^k(t) \end{bmatrix}.\end{aligned} \tag{20}$$

The *Poincaré-Ljapunov constant* (PLC) can be expressed directly with the help of the coefficients from (20) [7]

$$\begin{aligned}\Delta(\omega) = &\frac{1}{8\omega}(a_{20}+a_{02})(-a_{11}+b_{20}-b_{02})\\ &+\frac{1}{8\omega}(b_{20}+b_{02})\,(a_{20}-a_{02}+b_{11})\\ &+\frac{1}{8}(3a_{30}+a_{12}+b_{12}+3b_{03}).\end{aligned} \tag{21}$$

If $\Delta(\omega) > 0$ then the *Hopf bifurcation* is subcritical, otherwise, it is supercritical. Since the PLC can be calculated along the lobes as a function of the vibration frequency ω, we can follow the criticality of the *Hopf bifurcation* along the lobes. If we substitute the coefficients a_{jk}, b_{jk}, (20) we obtain

$$\Delta(\omega) = \frac{(\omega^2-1)^2}{w(\omega)}\,\frac{\delta_{n1}(\omega)\eta_2^2+\delta_{n2}(\omega)\eta_3}{u_d(\omega)\gamma_d(\omega)}. \tag{22}$$

where

$$\begin{aligned}\delta_{n1}(\omega) = &16\kappa\omega^2\,(48\kappa^5\tau(\omega)\omega^4+48\kappa^4\omega^2(\omega^2-1))\\ &+384\kappa^4\tau(\omega)\,\omega^4(\omega^2-1)^2\\ &+48\kappa^2\tau(\omega)\omega^2(\omega^2-1)^4\\ &+64\kappa^3\omega^2(\omega^2-1)^2(1+17\omega^2)\\ &-32\kappa\omega^2(\omega^2-1)^4(4\omega^2-1),\end{aligned} \tag{23}$$

$$\begin{aligned}\delta_{n2}(\omega) &= 3u_d(\omega)\gamma_n(\omega)(\omega^2-1),\\ u_d(\omega) &= 36\kappa^2\omega^2+(\omega^2-1)^2(4\omega^2-1)^2,\end{aligned} \tag{24}$$

and $\gamma_n(\omega)$, $\gamma_d(\omega)$ can be found in (15), (16).

We can determine the first harmonic component of the arising periodic motion analytically. Its amplitude can be expressed as a function of the bifurcation parameter w:

$$\begin{aligned}r(\omega,w) &= \sqrt{-\frac{\gamma(\omega)}{\Delta(\omega)}(w-w(\omega))}\\ &= \sqrt{2}\sqrt{1-\frac{w}{w(\omega)}}\sqrt{\frac{w(\omega)\gamma_n(\omega)u_d(\omega)}{\delta_{n1}(\omega)\eta_2^2+\delta_{n2}(\omega)\eta_3}}.\end{aligned} \tag{25}$$

This period one branch gives us a good approximation in for actual chip width values w close enough to the critical value $w(\omega)$.

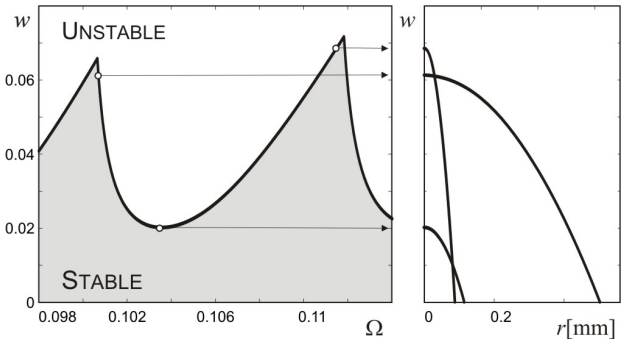

Figure 5: Structure of periodic orbits; j=10, κ = 0.01.

5 THE CRITICALITY OF THE HOPF BIFURCATION

It has great technical relevance what kind of limit cycle exists in the vicinity of the stability boundaries, that is, whether the arisen *Hopf bifurcation* is subcritical or supercritical. In the subcritical case, an unstable oscillation exists around the stable stationary cutting, which can still lead to chatter for perturbations larger than the amplitude of the unstable oscillation. Consequently the sign of (22) refers to the nature of the stability. Since the chatter frequencies $\omega \in (1,\infty)$ along the stability boundaries, $w(\omega)$, $\gamma_d(\omega)$ and $u_d(\omega)$ are positive in (22) in accordance with (13), (16) and (24). Thus, the sense of the bifurcation depends only on the nominator of the PLC, more exactly on the signs of $\delta_{n1}(\omega)$ defined in (23) and η_3 defined in (5):

$$\delta_{n1}(\omega)\eta_2^2+\delta_{n2}(\omega)\eta_3 > 0\,.$$

This way, we get the condition

$$\eta_3 > -\frac{\delta_{n1}(\omega)}{\delta_{n2}(\omega)}\,\eta_2^2\,, \tag{26}$$

Substituting (5) into the condition (26), the problem leads to a second order polynomial condition with respect to the theoretical chip thickness h_0:

$$\left(1+3\frac{\delta_{n1}(\omega)}{\delta_{n2}(\omega)}\right)\left(h_0^2+\frac{2}{3}\frac{\rho_2}{\rho_3}h_0\right)+\frac{\rho_1}{3\rho_3}+\frac{1}{3}\frac{\delta_{n1}(\omega)}{\delta_{n2}(\omega)}\frac{\rho_2^2}{\rho_3^2} > 0.$$

This condition is always satisfied if it has no real root for h_0, that is, if the discriminant D satisfies

$$D = -\rho_3\left(\rho_1-\frac{1}{3}\frac{\rho_2^2}{\rho_3}\right)\left(3\frac{\delta_{n1}(\omega)}{\delta_{n2}(\omega)}+1\right) < 0\,.$$

Since $\rho_3 > 0$ for all reasonable cutting force characteristics (2) and the last factor is always positive for all $\omega \in (1,\infty)$, $\kappa \in [0,\infty)$, we are left the simple condition

$$3\rho_1\rho_3 > \rho_2^2\,.$$

This condition is equivalent with the condition of the positive gradient at the inflection point (3) since

$$\frac{\partial F_x}{\partial h}(h_{\inf}) = z_C w\left(\rho_1-\frac{1}{3}\frac{\rho_2^2}{\rho_3}\right) > 0 \;\Leftrightarrow\; 3\rho_1\rho_3 > \rho_2^2\,.$$

Thus, if the gradient of the cubic cutting force function at the inflection point is positive, then the *Hopf bifurcation* is subcritical. Otherwise, the subcriticality is not proven mathematically, but again, having negative derivative at a possible inflection point on the cutting force characteristic is physically unreasonable.

6 ZONES OF BI-STABILITY

As explained above, the subcriticality of the *Hopf bifurcation* means that the unstable limit cycle separates two coexisting stable motions, the desired stable stationary cutting and the undesired large amplitude chatter that is also stable in the sense of dynamical systems theory. This is why this region is called the region of bi-stability. Since we proved that the *Hopf bifurcation* is subcritical along the lobes, the bi-stable regions are located below these lobes, covering a large region of the parameter domain of stable stationary cutting.

6.1 Bi-stable limits

According to (25) the first harmonic component of the limit cycle can be calculated as a projection of the real orbit to the subspace tangent to the centre manifold (Figure 4):

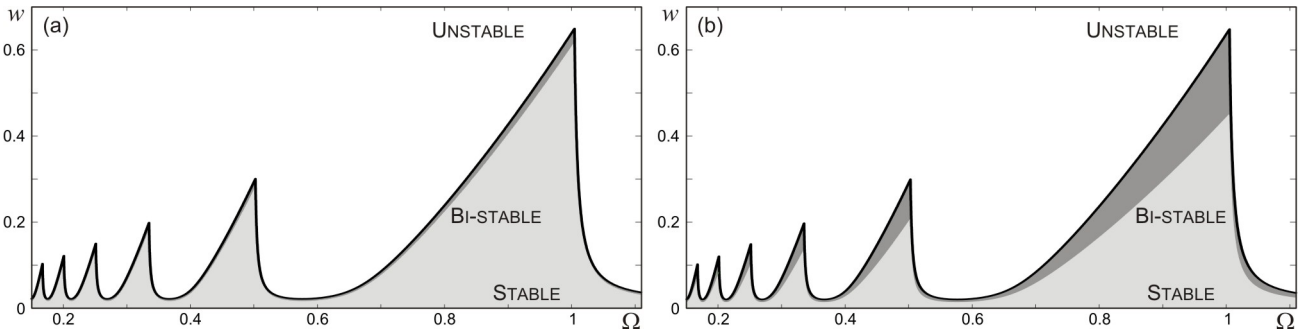

Figure 6: Both panels show the stability chart with the bi-stable region in case of the 3/4 power-law (a) and *Tobias cubic curve* (b); h_0=0.06 [mm], κ= 0.01.

$$\begin{bmatrix} z_1(t) \\ z_2(t) \\ \hdashline \mathbf{v}_t(\theta) \end{bmatrix} \approx \begin{bmatrix} r(\omega, w)\cos\omega t \\ -r(\omega, w)\sin\omega t \\ \hdashline \mathbf{0} \end{bmatrix}.$$

This way, the actual chip thickness is given by (4):

$$h(t) = y_{t,1}(-\tau) - y_{t,1}(0) + h_0 = -\frac{r(\omega, w)}{w(\omega)}\sqrt{(\omega^2-1)^2 + 4\kappa^2\omega^2}\cos(\omega t + \delta) + h_0 .$$

The tool leaves the surface of the work-piece when the chip thickness becomes zero:

$$h(t) = 0 \quad \Rightarrow \quad \frac{r(\omega, w)}{w(\omega)}\sqrt{(\omega^2-1)^2 + 4\kappa^2\omega^2} = h_0 . \qquad (27)$$

If we project this condition (27) onto the plane spanned by ($y_{t,1}(-\tau)$, $y_{t,1}(0)$), that is by ($x(t-\tau)$, $x(t)$) as shown in Figure 7, we obtain a straight-line as switching condition. The tool leaves the surface of the work-piece when the orbits shown as ellipses in Figure 7 hit this switching line.

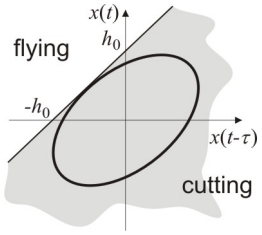

Figure 7: Critical periodic orbit in reduced phase space.

Expressing the bifurcation parameter w from (27), we get the so-called bi-stable limit where the periodic orbits reach the switching line:

$$w_{bs}(\omega) = w(\omega)\left(1 - \frac{1}{4}\frac{h_0^2}{\omega^2 - 1}\frac{\delta_{n1}(\omega)\eta_2^2 + \delta_{n2}(\omega)\eta_3}{\gamma_n(\omega)u_d(\omega)}\right).$$

7 CONCLUSION

Figure 6 shows the bi-stable regions as dark strips in the grey stable cutting domain, just below the white unstable parameter domain. With the appropriate choice of the parameters η_2, η_3 from (6), the results are shown for both 3/4 law and for the *Tobias cubic curve*.

While the dimensionless linear stability boundary is not affected at all by the applied cutting force characteristic function, the size of the bi-stable region strongly depends on it. Clearly, this bi-stable region is much larger if the cutting force characteristics follow the cubic curve rather than the power-law.

During the design of the technological parameters, it is much more convenient and common to use the power-law approximation of the real measured cutting force characteristics. From the view-point of the stability prediction of the stationary cutting the linearization of this power-law is still appropriate. However, from nonlinear vibrations view-point, the use of the power-law approximation has great deficiencies. As we showed, the prediction of the bi-stable parameter domain is important if we want to secure stable stationary cutting robust enough for perturbations. However, this domain cannot be predicted correctly, in a conservative way, if we use the power-law approximation.

We proved that the *Tobias cubic curve* approximation of the cutting force characteristics leads to subcritical *Hopf bifurcations* along all the stability limits in the same way as it was shown for the power-law by [4]. In the meantime we also showed that the bi-stable domain can be substantially larger for these cutting force characteristics than one predicted by the power-law.

8 REFERENCES

[1] Altintas, Y., Budak, E., 1995, Analytical prediction of stability lobes in milling, CIRP, 44(1), **pp**. 357-362.

[2] Dombóvári, Z., 2006, Bifurcation analysis of a cutting process, MSc. thesis, BUTE, Hungary.

[3] Insperger, T., Stépán, G., Bayly, P.V., Mann, B. P., 2003, Multiple chatter frequencies in milling processes, Journal of Sound and Vibration 262, **pp**. 333-345.

[4] Kalmár-Nagy, T., Pratt, R. J., 1999, Experimental and analytical investigation of the subcritical instability in metal cutting, ASME, Nevada, USA.

[5] Kienzle, O., 1957, Spezifische Schnittkräfte bei der Metallbearbeitung, Werkstattstechnik und Maschinenbau, 47.

[6] Shi, H. M., Tobias, S. A., 1984, Theory of finite amplitude machine tool instability, Int. J. of Machine Tool Design and Research, 24, **pp**. 45-69.

[7] Stépán, G., 1989, Retarded Dynamical Systems, Longman, London.

[8] Stépán, G., Kalmár-Nagy, T., 1997, Nonlinear Regenerative Machine Tool Vibrations, ASME, California, USA.

[9] Szalai, R., Stépán, G., Hogan, S. J., 2004, Global dynamics of low immersion high-speed milling, Chaos(14), **pp**. 1069-1077.

[10] Taylor. F.W., 1907, On the art of cutting metals. Transaction of ASME, 28:31–350.

[11] Tlusty, J., Spacek, L., 1954, Self-Excited Vibrations on Machine Tools (in Czech), Nakl CSAV, Prague.

[12] Tobias, S. A., 1965, *Machine Tool Vibrations*, Blackie, London.